Journal of Magnetic Resonance 305 (2019) 175–179

Contents lists available at ScienceDirect

Journal of Magnetic Resonance

journal homepage: www.elsevier.com/locate/jmr

Detecting acetylated aminoacids in blood serum using hyperpolarized ^{13}C-^{1}H-2D-NMR

Sotirios Katsikis [a], Ildefonso Marin-Montesinos [b], Christian Ludwig [c], Ulrich L. Günther [d,*]

[a] Department of Pharmacognosy and Natural Products Chemistry, School of Pharmacy, National and Kapodistrian University of Athens, Athens, Greece
[b] CICECO—Chemistry Department, University of Aveiro, Campus de Santiago, 3810-193 Aveiro, Portugal
[c] Institute of Metabolism and Systems Research, University of Birmingham, Birmingham, UK
[d] HWB-NMR, University of Birmingham, Institute of Cancer and Genomic Sciences, University of Birmingham, Birmingham, UK

ARTICLE INFO

Article history:
Received 14 February 2019
Revised 4 July 2019
Accepted 4 July 2019
Available online 5 July 2019

Keywords:
DNP
Dynamic nuclear polarization
Aminoacids
Metabolism

ABSTRACT

Dynamic Nuclear Polarization (DNP) can substantially enhance the sensitivity of NMR experiments. Among the implementations of DNP, ex-situ dissolution DNP (dDNP) achieves high signal enhancement levels owing to a combination of a large temperature factor between 1.4 and 300 K with the actual DNP effect in the solid state at 1.4 K. For sufficiently long T_1 relaxation times much of the polarization can be preserved during dissolution with hot solvent, thus enabling fast experiments during the life time of the polarization. Unfortunately, for many metabolites found in biological samples such as blood, relaxation times are too short to achieve a significant enhancement. We have therefore introduced ^{13}C-carbonyl labeled acetyl groups as probes into amino acid metabolites using a simple reaction protocol. The advantage of such tags is a sufficiently long T_1 relaxation time, the possibility to enhance signal intensity by introducing ^{13}C, and the possibility to identify tagged metabolites in NMR spectra. We demonstrate feasibility for mixtures of amino acids and for blood serum. In two-dimensional dDNP-enhanced HMQC experiments of these samples acquired in 8 s we can identify acetylated amino acids and other metabolites based on small differences in chemical shifts.

1. Introduction

The dissolution Dynamic Nuclear Polarization (dDNP) experiment pioneered by Ardenkjær-Larsen et al. [1] can achieve signal enhancements at the order of magnitude of 10,000-fold, for nuclei with low gyromagnetic ratios such as ^{13}C and ^{15}N. These large enhancements arise from a combination of a temperature factor (for polarizations at temperatures <1.5 K and dissolution to room temperature) and the actual DNP effect [2–4]. The requirements of freezing the sample in a glass state and dissolving with hot solvent in order to transfer it to an NMR magnet for spectrum acquisition limits the selection of molecules amenable to this approach to those with sufficiently long T_1 relaxation times. Dissolution DNP has gained considerable importance as it forms the basis for what is now often termed chemical shift metabolic imaging [5], mainly using pyruvate as the polarization carrier. The limiting factors for dissolution DNP are the relatively long polarisation time and the need to carry out the experiment within the short time frame of the T_1 relaxation time of the analyte. As a consequence, a variety of systems were implemented with the ultimate goal of eliminating sample transfer time, either by using a pressurised sample delivery system [6,7], by using dual-centre magnets [8] or recently by a solid pellet driven sample transfer approach [9]. Such implementations have enabled applications in protein folding and reaction monitoring [10–13].

There have been several approaches to design probes with long life times which can preserve polarization over an extended period of time. For example, very long life-times are achieved for some ^{15}N-bearing probes. Considerable research has been carried out to identify molecules with long-lived spin states, some have life-times greater than 15 min [14–17]. However, only few probes can be attached to other molecules and are suitable to identify different molecules as part of a mixture in NMR experiments. This is where formyl and acetyl tags possess a significant advantage. As shown by Raftery and co-workers [18] the combined methyl-proton and ^{13}CO chemical shifts of N-acetyl-tags have sufficient dispersion to distinguish 20 amino acids in a 'long-range' HSQC spectrum utilizing the small $^{2}J_{CH}$ coupling constant between the methyl protons and the ^{13}CO. Wilson et al. showed the utility of ^{13}C-labeled acetyl probes in conjunction with dDNP for one-dimensional spectra of glycine, serine, valine and alanine [19].

* Corresponding author.
E-mail address: u.l.gunther@bham.ac.uk (U.L. Günther).

https://doi.org/10.1016/j.jmr.2019.07.003
1090-7807/

The life-time of acetyl groups is sufficiently long for dDNP experiments ($T_1 \approx 40$ s), especially when fast transfer systems such as high-pressure dissolution devices are used [15]. The T_1 of the acetyl group is longer than that of the other ^{13}C-nuclei in amino acids, although shorter than typical long-lived tags [14–17]. Here we show how acetyl probes can be used to obtain two-dimensional ^{13}C-observed HMQC spectra after polarization of mixtures of acetylated amino acids. We also show that the dDNP approach yields sufficient sensitivity to identify a range of common amino acids in bovine blood serum after acetylating NH- and OH-bearing molecules in serum using ^{13}C-labeled acetyl tags.

2. Implementation

In order to evaluate the suitability of acetyl-tags to analyze mixtures of metabolites using dDNP, we first used two test samples comprising a mixture of amino acids, and also applied the acetylation procedure directly to fetal bovine blood serum. As initial test samples we used mixtures of 5 and 20 amino acids. Samples were acetylated using a simple and fast reaction where ^{13}C-labeled acetic anhydride is used to attach tags to NH_2 groups of amino acids (see Section 4). This reaction can be carried out to achieve virtually complete acetylation of all NH groups [18]. The ^{13}CO along with the methyl protons can be used for long-range ^{1}H-^{13}C-HSQC or HMQC spectra based on the small $^{2}J_{CH}$ coupling constant of ~7 Hz. In such spectra one signal is observed per amino acid, except for amino acids with side chains NH_2 groups, such as lysine where a second signal will be observed.

3. Results and discussion

A long-range ^{13}C-^{1}H-HMQC spectrum for the N-acetylated amino acids glycine, threonine, valine, alanine and proline, obtained after 3 h of polarizing ^{13}C using the OX63 trityl radical, followed by fast dissolution, shows all the expected signals with assignments taken from [18] (Fig. 1A). The acquisition of the HMQC spectrum was carried out as described earlier [20] with ^{13}C in the direct, and ^{1}H in the incremented dimension, using a small flip angle HMQC sequence that preserves z-magnetization between increments (Fig. 1B, see Section 4 for details). For acetyl groups the ^{13}CO-signal of the acetyl group is acquired followed by a transfer to protons and then back to ^{13}C for acquisition using the pulse sequence shown in Fig. 1B. Decoupling can be used without destroying polarisation and fractions of the available polarisation can be read out for each increment of the 2D-experiment. All dDNP spectra were rotated by 90° to show the incremented ^{1}H-axis in the horizontal direction in order to be directly comparable to a conventional HSQC spectrum. An equally good result was obtained for a mixture of all 20 amino acids as shown in Fig. 2B. In this spectrum most of the signals could be assigned by comparing chemical shifts previously reported by Shanaiah et al [18]. There is also reasonably good agreement between this spectrum and an analogous conventional thermal ^{1}H-^{13}C-HSQC spectrum (acquired in 40 min) (Fig. 2A), although resolution is not as good in the 10sec dDNP enhanced spectrum which makes it difficult to compare the two for all signals. The dDNP spectrum shows also one extra signal at 177 pm/1.35 ppm (labeled *) which is likely a side chain CO of glutamate and some signals seem to be shifted and can therefore not be assigned by comparing chemical shifts. There are also some signals missing in the dDNP spectrum, specifically signals for phenylalanine (F) and tyrosine (Y), although the second signal for Y is present. Some differences may be explained by lack of temperature stability and the presence of the radical. Considering that it is aromatic aminoacids that we don't observe an interaction with the radical is the most likely cause, especially considering that self-assembly and interaction with other molecules has already been shown for the OX63 radical that has also been used in this work [21,22].

In order to assess whether the method could be generalized to real biological samples, we applied the methodology to fetal bovine blood serum. When acetylating blood serum, proteins had to be removed to avoid acetylation of protein amino acids, which would limit the yield of acetylation for small molecules, as the anhydrite also reacts with amino acids in proteins in which reduces the yield of acetylated small molecules (see Section 4). A 2D-^{13}C-^{1}H-HMQC spectrum acquired after dDNP in 8 s after polarization at 1.4 K for 2–3h is shown in Fig. 2D. There is good agreement between this spectrum and an analogous convention thermal ^{1}H-^{13}C-HSQC spectrum (Fig. 2C). It should be noticed that the sample concentration in the thermal sample was 80 times higher than in the DNP sample.

Although conventionally acquired HSQC spectra can easily be acquired with longer acquisition times at a higher resolution, this work demonstrates the potential of dDNP in the context of small molecule mixture analysis. Metabolomics and DNP-NMR are fast developing fields [4] and there are several alternative methods to obtain fast HSQC or HMQC spectra, the most commonly used being the ultra-fast sequence [2,23]. We chose the small flip-angle HMQC as it is less demanding on hardware and can be carried out using conventional heteronuclear NMR probes.

The use of acetyl tags largely eliminates one of the biggest disadvantages of dDNP, where intensities are scaled by the T_1 of the hyperpolarized nucleus in the dissolution buffer. Considering the similarity of structure and small difference in size between amino acids we expect minimal differences in T_1 of the acetyl tag after dissolution. At the same time the chemical shift dispersion is sufficient to identify all natural amino acids, even with low resolution spectra.

While this work demonstrates the applicability of dDNP for typical metabolomics applications, the limiting factor is in the long polarization times which can be overcome by a number of options, including polarization via protons or parallel polarization of multiple nuclei specimen. Even though a conventional HSQC would be preferable at this point, it is increasingly clear that dDNP will play a role for specific applications, and the use of the acetylation method described here in the context of dDNP could be of significant value for real-time cell-based experiments that are currently being developed in many labs [25–27], and also in the context of using micro-detection NMR where ultimate sensitivities are of paramount importance [28,29].

4. Experimental

4.1. Preparation of acetylated samples

We prepared three samples to be tagged with ^{13}C-labeled acetyl groups: (i) a 5 aminoacid mixture to help calibrate the experimental conditions, (ii) a 20 aminoacid mixture to prove that an analysis of a relatively complex mixture is possible using dDNP and finally (iii) a sample of acetylated deproteinated bovine serum to prove that the method is applicable to more complex biological samples. Our sample preparation is based on a previously published protocol [18]. The exact sample preparation for each is described below.

Initially 100 mM stock solutions were prepared for all amino acids. For the mix of 5 amino acids 200 μL were taken from each stock solution (total volume 1 mL) and 20 μL of acetic anhydride-1,1′-$^{13}C_2$ were added while constantly adjusting the pH under stirring for 30 min to the value of 8. Subsequently, the sample was lyophilised and reconstituted in 1 mL of D_2O to reach a final concentration of 20 mM for each amino acid. For the DNP experiment this was further diluted 1:1 with DMSO d_6 to achieve a glass

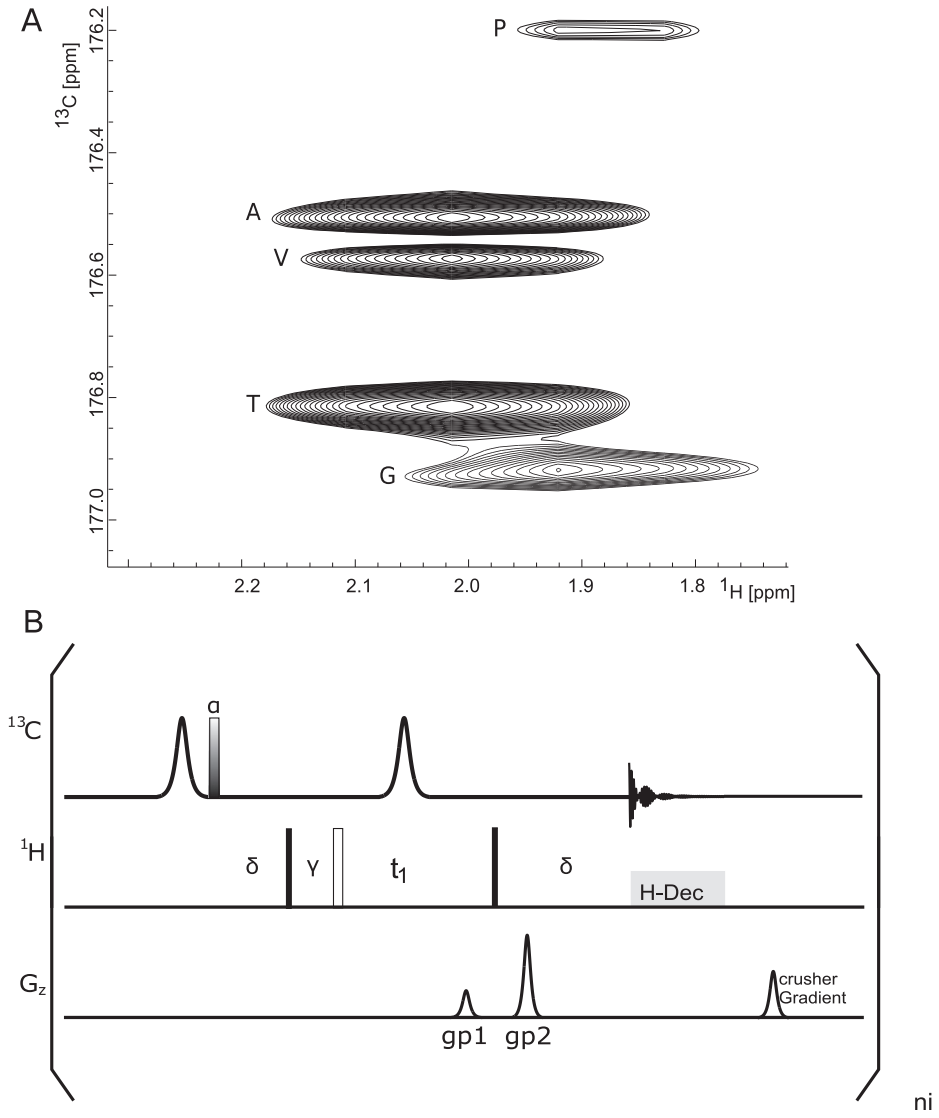

Fig. 1. A. ^{13}C–^{1}H-FAST-HMQC dDNP spectrum of standard sample containing the N-acetylated amino acids glycine (G), threonine (T), valine (T), alanine (A) and proline (P), acquired using the pulse sequence in panel B, where ^{13}C was observed and ^{1}H incremented. **B.** Small flip-angle HMQC sequence used for data acquisition of DNP spectra. In this sequence z-magnetization is preserved between increments and a small portion is read out by a small flip angle for every increment (pulse labeled α). The solid rectangular pulses are 90° hard pulses, and the adiabatic 180° ^{13}C pulse (γ) had a hyperbolic secant shape with the pulse length set to 1 ms to avoid losses arising from B_1 field inhomogeneity. The HMQC delay δ gave optimal S/N at 1/(2 * 7 Hz) for the long-range $^{2}J_{CH}$ coupling from the methyl-^{1}H to the carbonyl-^{13}C. Pulsed field selection gradients gp1 and gp2 of 1 ms were executed at relative power levels (gp1 * ($\gamma_C - \gamma_H$) = gp2 * γ_C), i.e. gp1:gp2 = 1:3 (22%/66%). The crusher gradient was of arbitrary strength (45%).

state, i.e. the final concentration in the cup was 10 mM. Of this 100 μL were put in the polarizer, yielding a concentration of 250 μM for each aminoacid after dissolution with 4 mL of hot solvent.

For the mixture of 20 amino acids the procedure was similar: 10 μL of amino acid was taken leading to a final volume of 200 μL; 40 μL of acetic anhydride-1,1′-$^{13}C_2$ were added to produce the labeled sample. Both samples containing the acetylated amino acids had a dissolved concentration of 250 μM for each of the 20 standard amino acids.

The acetylated serum sample was prepared by taking 10 mL of FBS (PAA, Fetal Bovine Serum Gold, EU approved) to which 50 mL of methanol was added to precipitate proteins. After spinning down precipitated proteins for 15 min at 10.000 rpm, another 50 mL of methanol were added, followed by an additional centrifugation step. These two steps were essential to avoid losses in small molecule acetylation. The supernatant was then passed through a 10 kDa molecular weight cut-off filter (pore size 5 nm). Subsequently the sample was lyophilized and then dissolved in D_2O. For DNP experiments 100 μL were pipetted into the DNP cup along with an equal amount of DMSO d_6. In order to maximise the dissolution efficiency, frozen beads were prepared by pipetting small amounts of material on a plate cooled with liquid nitrogen, just before inserting the cup in the polariser.

4.2. NMR and dissolution-DNP experimental details

Polarizations were carried out using a Hypersense® DNP polariser from Oxford Instruments. The optimal polarization frequency for ^{13}C was 94.090 GHz. The microwave power was set at 100 mW and the cryostat temperature was set at 1.4 K, polarization times were 2–3h. Dissolution was performed using a one to one mixture of methanol and water preheated at 463.15 K and pressurised to 9 bar. Radical used throughout the study was the OX63 trityl radical.

A ^{13}C-^{1}H-HMQC pulse sequence (Fig. 1B) with small flip angle incrementation (Fig. 1B), similar to the one previously published [20], was employed, which preserves magnetization on the z-axis

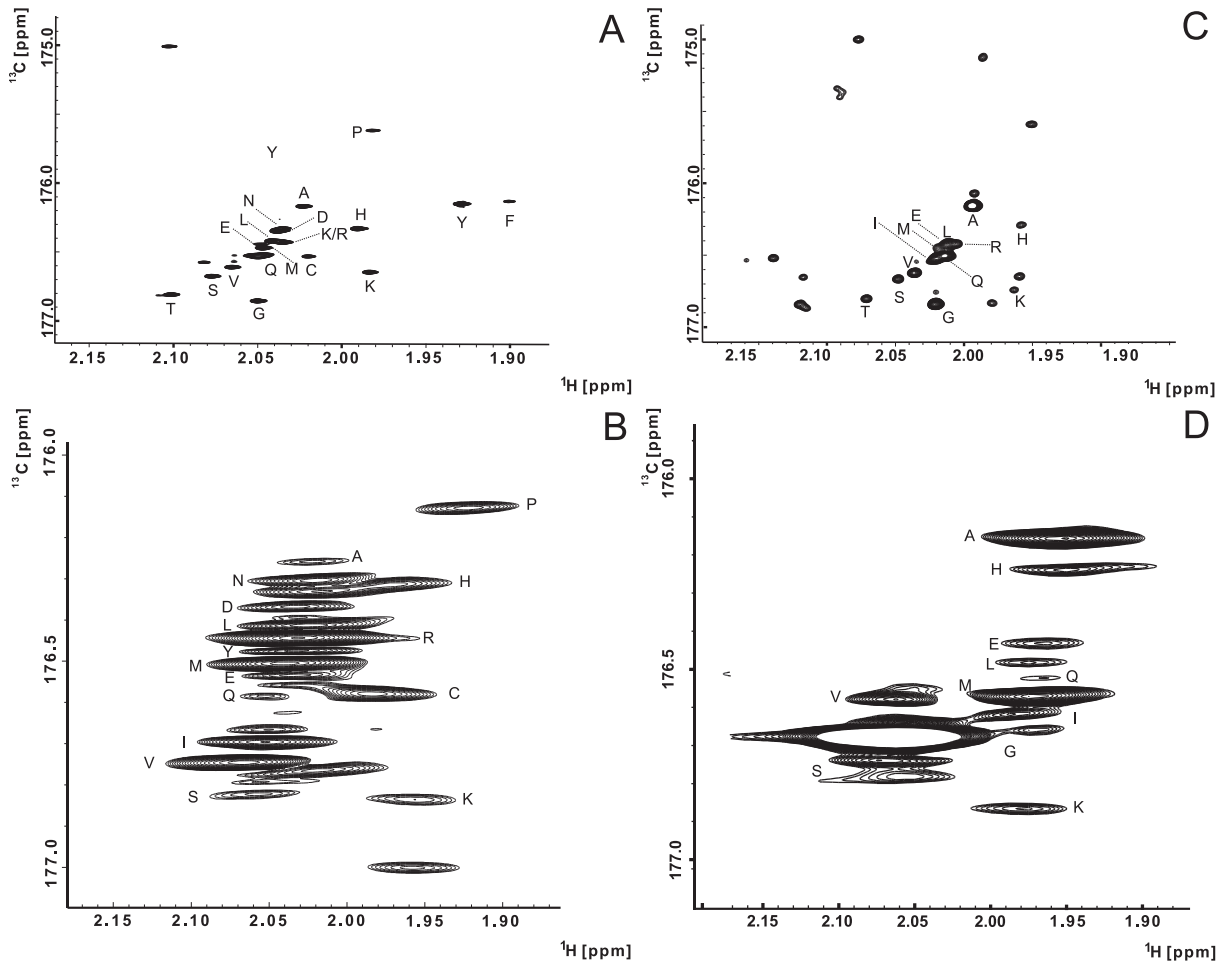

Fig. 2. A and C: Echo-antiecho long-range HSQC of a mixture of 20 ^{13}CO-acetylated amino acids (A), and ^{13}CO-acetylated serum (C). B&D: Respective dDNP small flip angle ^{13}C-^{1}H-HMQC [24] spectra of the same samples. Spectra in B&D were rotated, i.e. the incremented ^{1}H dimension is shown in horizontal direction for comparison with thermal HSQCs. (T, threonine, S, serine, V, valine, Y, tyrosine, E, glutamate, I, isoleucine, G, glycine, L, leucine, Q, glutamine, N, asparagine, M, methionine, A, Alanine, D, aspartate, K, lysine, C, cysteine, H, histidine, P, proline, F, phenylalanine and *unassigned signal).

between scans and reads out magnetization using subsequently small flip angles.

The acquisition time for the small flip-angle HMQC was 0.5 s per increment. The number of points was 512 in the direct dimension and we acquired 16 increments. The total NMR experiment time was 10 s, with the preacquisition delay set to 1.5–2 s. Preacquisition delay is the time needed between the timepoint of the Hypersense producing a trigger signal and the actual sample transfer being completed, and it varies with the transfer system. Using the in-house high pressure transfer system which we described here, optimal value for this solvent system was found to be 1.5 s. For the conventional dissolution system this value was optimised at 2 s, for this matrix. Therefore, the total acquisition time for the 16 increments was 9 s. The FIDs were zero-filled to 4 k points in the direct and 128 points in the indirect dimension. Transmitter offsets were set as 171.5 ppm for ^{13}C and 2.438 ppm for ^{1}H, respectively. Spectral widths were set to 4 and 0.4 ppm respectively. The in-house high-pressure transfer system is slightly faster, although for 50/50 methanol/water transfer the experiments can also be performed with the standard Hypersense® dissolution system.

Declaration of Competing Interest

The authors have no competing interest to declare.

Acknowledgements

Research leading to these results received funding from the European Commission in the context of the METAFLUX FP7 ITN project (264780). The authors would like to thank Oxford Instruments for hosting SK as a researcher as part of this grant and HWB-NMR for providing the support needed for the completion of this work. We are also grateful to the Wellcome Trust for supporting access to NMR instruments at the Henry Wellcome Building for Biomolecular NMR in Birmingham (grant number 208400/Z/17/Z).

References

[1] J.H. Ardenkjaer-Larsen, B. Fridlund, A. Gram, G. Hansson, L. Hansson, M.H. Lerche, R. Servin, M. Thaning, K. Golman, Increase in signal-to-noise ratio of >10,000 times in liquid-state NMR, Proc. Natl. Acad. Sci. 100 (2003) 10158–10163.

[2] L. Frydman, D. Blazina, Ultrafast two-dimensional nuclear magnetic resonance spectroscopy of hyperpolarized solutions, Nat. Phys. 3 (2007) 415–419, https://doi.org/10.1038/nphys597.

[3] U.L. Günther, Dynamic nuclear hyperpolarization in liquids, in: H. Heise, S. Matthews (Eds.), Modern NMR Methodology, Springer, Berlin Heidelberg, Berlin, Heidelberg, 2011, pp. 23–69 (accessed March 12, 2014).

[4] B. Plainchont, P. Berruyer, J.-N. Dumez, S. Jannin, P. Giraudeau, Dynamic nuclear polarization opens new perspectives for NMR spectroscopy in analytical chemistry, Anal. Chem. 90 (2018) 3639–3650, https://doi.org/10.1021/acs.analchem.7b05236.

[5] R. Hesketh, K.M. Brindle, Magnetic resonance imaging of cancer metabolism with hyperpolarized ^{13}C-labeled cell metabolites, Curr. Op. Chem. Biol. 45 (2018) 187–194, https://doi.org/10.1016/j.cbpa.2018.03.004.
[6] S. Katsikis, I. Marin-Montesinos, M. Pons, C. Ludwig, U.L. Günther, Improved stability and spectral quality in ex situ dissolution DNP using an improved transfer device, Appl. Magn. Reson. 46 (2015) 723–729, https://doi.org/10.1007/s00723-015-0680-5.
[7] S. Bowen, C. Hilty, Rapid sample injection for hyperpolarized NMR spectroscopy, PCCP 12 (2010) 5766–5770, https://doi.org/10.1039/C002316g.
[8] J. Leggett, R. Hunter, J. Granwehr, R. Panek, A dedicated spectrometer for dissolution DNP NMR spectroscopy, Phys. Chem. Chem. Phys. 12 (2010) 5883–5892.
[9] K. Kouřil, H. Kouřilová, S. Bartram, M.H. Levitt, B. Meier, Scalable dissolution-dynamic nuclear polarization with rapid transfer of a polarized solid, Nat Commun. 10 (2019) 1733, https://doi.org/10.1038/s41467-019-09726-5.
[10] T.C. Eisenschmid, R.U. Kirss, P.P. Deutsch, S.I. Hommeltoft, R. Eisenberg, J. Bargon, R.G. Lawler, A.L. Balch, Para hydrogen induced polarization in hydrogenation reactions, J. Am. Chem. Soc. 109 (1987) 8089–8091.
[11] J. Kim, M. Liu, H.-Y. Chen, C. Hilty, Determination of intermolecular interactions using polarization compensated heteronuclear overhauser effect of hyperpolarized spins, Anal. Chem. 87 (2015) 10982–10987, https://doi.org/10.1021/acs.analchem.5b02934.
[12] Y. Kim, C. Hilty, Affinity screening using competitive binding with fluorine-19 hyperpolarized ligands, Angew. Chem. Int. Ed. 54 (2015) 4941–4944, https://doi.org/10.1002/anie.201411424.
[13] M. Ragavan, L.I. Iconaru, C.-G. Park, R.W. Kriwacki, C. Hilty, Real-time analysis of folding upon binding of a disordered protein by using dissolution DNP NMR spectroscopy, Angew. Chem. Int. Ed. 56 (2017) 7070–7073, https://doi.org/10.1002/anie.201700464.
[14] J.-N. Dumez, B. Vuichoud, D. Mammoli, A. Bornet, A.C. Pinon, G. Stevanato, B. Meier, G. Bodenhausen, S. Jannin, M.H. Levitt, Dynamic nuclear polarization of long-lived nuclear spin states in methyl groups, J. Phys. Chem. Lett. 8 (2017) 3549–3555, https://doi.org/10.1021/acs.jpclett.7b01512.
[15] H. Nonaka, R. Hata, T. Doura, T. Nishihara, K. Kumagai, M. Akakabe, M. Tsuda, K. Ichikawa, S. Sando, A platform for designing hyperpolarized magnetic resonance chemical probes, Nat Commun. 4 (2013) 2411, https://doi.org/10.1038/ncomms3411.
[16] H. Nonaka, M. Hirano, Y. Imakura, Y. Takakusagi, K. Ichikawa, S. Sando, Design of a 15N molecular unit to achieve long retention of hyperpolarized spin state, Sci. Rep. 7 (2017) 40104, https://doi.org/10.1038/srep40104.
[17] P.R. Vasos, A. Comment, R. Sarkar, P. Ahuja, S. Jannin, J.-P. Ansermet, J.A. Konter, P. Hautle, B. Van den Brandt, G. Bodenhausen, Long-lived states to sustain hyperpolarized magnetization, Proc. Natl. Acad. Sci. 106 (2009) 18469–18473.
[18] N. Shanaiah, M.A. Desilva, G.A. Nagana Gowda, M.A. Raftery, B.E. Hainline, D. Raftery, Class selection of amino acid metabolites in body fluids using chemical derivatization and their enhanced 13C NMR, Proc. Natl. Acad. Sci. 104 (2007) 11540–11544, https://doi.org/10.1073/pnas.0704449104.
[19] D.M. Wilson, R.E. Hurd, K. Keshari, M. Van Criekinge, A.P. Chen, S.J. Nelson, D.B. Vigneron, J. Kurhanewicz, Generation of hyperpolarized substrates by secondary labeling with [1, 1–13C] acetic anhydride, Proc. Natl. Acad. Sci. 106 (2009) 5503–5507.
[20] C. Ludwig, I. Marin-Montesinos, M.G. Saunders, A.-H. Emwas, Z. Pikramenou, S. P. Hammond, U.L. Günther, Application of ex situ dynamic nuclear polarization in studying small molecules, PCCP 12 (2010) 5868, https://doi.org/10.1039/c002700f.
[21] I. Marin-Montesinos, J.C. Paniagua, M. Vilaseca, A. Urtizberea, F. Luis, M. Feliz, F. Lin, S. Van Doorslaer, M. Pons, Self-assembled trityl radical capsules – implications for dynamic nuclear polarization, Phys. Chem. Chem. Phys. 17 (2015) 5785–5794, https://doi.org/10.1039/C4CP05225K.
[22] I. Marin-Montesinos, J.C. Paniagua, A. Peman, M. Vilaseca, F. Luis, S. Van Doorslaer, M. Pons, Paramagnetic spherical nanoparticles by the self-assembly of persistent trityl radicals, Phys. Chem. Chem. Phys. 18 (2016) 3151–3158, https://doi.org/10.1039/C5CP05767A.
[23] P. Giraudeau, L. Frydman, Ultrafast 2D NMR: an emerging tool in analytical spectroscopy, Annual Rev. Anal. Chem. 7 (2014) 129–161, https://doi.org/10.1146/annurev-anchem-071213-020208.
[24] C. Ludwig, I. Marin-Montesinos, M.G. Saunders, U.L. Günther, Optimizing the polarization matrix for ex situ dynamic nuclear polarization, J. Am. Chem. Soc. 132 (2010) 2508–2509, https://doi.org/10.1021/ja909984w.
[25] T. Harris, H. Degani, L. Frydman, Hyperpolarized ^{13} C NMR studies of glucose metabolism in living breast cancer cell cultures, NMR Biomed. 26 (2013) 1831–1843, https://doi.org/10.1002/nbm.3024.
[26] S. Meier, P.R. Jensen, J.Ø. Duus, Real-time detection of central carbon metabolism in living *Escherichia coli* and its response to perturbations, FEBS Lett. 585 (2011) 3133–3138, https://doi.org/10.1016/j.febslet.2011.08.049.
[27] S. Jeong, R. Eskandari, S.M. Park, J. Alvarez, S.S. Tee, R. Weissleder, M.G. Kharas, H. Lee, K.R. Keshari, Real-time quantitative analysis of metabolic flux in live cells using a hyperpolarized micromagnetic resonance spectrometer, Sci. Adv. 3 (2017), https://doi.org/10.1126/sciadv.1700341 e1700341.
[28] A. Yilmaz, M. Utz, Characterisation of oxygen permeation into a microfluidic device for cell culture by in situ NMR spectroscopy, Lab Chip 16 (2016) 2079–2085, https://doi.org/10.1039/C6LC00396F.
[29] G. Finch, A. Yilmaz, M. Utz, An optimised detector for in-situ high-resolution NMR in microfluidic devices, J. Magn. Reson. 262 (2016) 73–80, https://doi.org/10.1016/j.jmr.2015.11.011.